

Preparation and Characterization of Regenerated Cellulose Biocomposite Film Filled with Calcium Carbonate by *in situ* Precipitation

Qianqian Zhu,^{a,d} Jingjing Wang,^a Jianzhong Sun,^{a,*} and Qianqian Wang^{a,b,c,*}

The application of cellulose hybrid biocomposites filled with calcium carbonate has attracted wide attention in packaging and other fields in recent years. In this study, regenerated cellulose (RC) films filled with calcium carbonate were successfully prepared by dissolution, regeneration, and *in situ* precipitation of CaCO₃. The optical, mechanical, physical, and chemical properties of biocomposites were examined by UV-visible spectroscopy, tensile testing, scanning electron microscopy (SEM), X-ray diffraction (XRD), Fourier transform infrared spectroscopy (FTIR), and thermogravimetric analyses (TGA). The results showed that RC films with different CaCO₃ contents exhibited good flexibility, optical properties, mechanical strength, and thermal stability. The RC biocomposite filled with calcium carbonate showed a tensile strength of 84.7 ± 1.5 MPa at optimum conditions. These RC biocomposites filled with CaCO₃ may find application in packaging.

Keywords: Organic-inorganic hybrid biocomposite; Calcium carbonate; Mechanical property; Characterization

Contact information: a: Biofuels Institute, School of the Environment and Safety Engineering, Jiangsu University, Zhenjiang 212013 China; b: State Key Laboratory of Pulp and Paper Engineering, South China University of Technology, Guangzhou 510640 China; c: Institute of Chemical Industry of Forest Products, Chinese Academy of Forestry, Key Laboratory of Biomass Energy and Material, Jiangsu Province, Nanjing 210042, China; d: Analysis and Testing Center, Jiangsu University, Zhenjiang, 212013 PR China; *Corresponding authors: jzsun1002@ujs.edu.cn; qianqian.wz@gmail.com

INTRODUCTION

As a renewable, biodegradable, and biocompatible polymer, cellulose offers tremendous opportunities for different products, including paper and paperboard, textiles, and drug tablets (Wang *et al.* 2018, 2019; Zhu *et al.* 2020a,b). Although it is generally considered as abundant and low-cost biomass, the price of the cellulose pulp is still high compared with inorganic fillers (Laukala *et al.* 2017; Xu *et al.* 2017). Inorganic fillers, such as calcium carbonate, are used in nearly every paper and paperboard product to save virgin pulp, dry energy, and production costs. The addition of CaCO₃ also brings some special properties for the final paper products, such as optical, physical, mechanical, and surface property improvements (Cheng *et al.* 2016; Seo *et al.* 2017; Choi *et al.* 2018). Ground and precipitated calcium carbonate fillers (GCC and PCC, respectively) are normally added to the cellulose pulp suspension before the formation of paper or paperboard. *In-situ* CaCO₃ formation can be also applied with the aim of maximizing filler retention (Ciobanu *et al.* 2010; Seo *et al.* 2017). Biomimetic design and synthesis of nanocellulose-CaCO₃ hybrid materials to new green materials are also in the spotlight (Saito *et al.* 2014; Nakao *et al.* 2019). Biodegradable regenerated cellulose (RC) films can be prepared by coagulation and

regeneration from various cellulose solvents, including ionic liquids (ILs), N,N-dimethylacetamide/lithium chloride (DMA/LiCl), and NaOH/urea solution (Sathitsuksanoh *et al.* 2013; Wang *et al.* 2016). The obtained RC films showed much better properties, such as better air oxygen permeability, thermal stability, and lower thermal expansion coefficient, compared to petroleum-based plastic substrates. The RC films show great potential in packaging and other applications. To further improve the performance of cellulose films, biodegradable cellulose copolymer films with organic fillers/coatings were prepared (Delhom *et al.* 2010; Yang *et al.* 2014).

However, the research on *in situ* precipitation of calcium carbonate on RC films is limited. The precipitation behavior of CaCO₃ on RC film from the ionic liquid (1-butyl-3-methylimidazolium chloride, BMIMCL) in ethanol-water was presented by Xiao *et al.* (2011), while the mineralization of CaCO₃ on RC film from DMA/LiCl solvent was investigated by Rauch *et al.* (2012). The mechanism for *in situ* calcium carbonate precipitation in RC hydrogel was proposed by Rauch *et al.* (2012). It is well known that cellulose surfaces are negatively charged, thus leading to accumulation of Ca²⁺ ions in the charged surface and inducing the nucleation, aggregation, and crystallization. The crystallization of calcium carbonate is limited to the specific nucleation sites, because of the complexation of the Ca²⁺ ions and negatively charged groups in cellulose fibers. The nanocrystals then grow larger and the small aggregates are formed, and these are interconnected by the cellulose fibers. Subsequently, these crystals that are strongly attached to the cellulose network become assembled into large aggregates. To the authors' best knowledge, there is no report on the *in situ* precipitation of calcium carbonate on regenerated cellulose made from NaOH/urea solution. Little is known about the effects of calcium carbonate when incorporated into the RC matrix by *in situ* precipitation. As an inorganic filler, the incorporation of calcium carbonate could lead to an improvement in biocomposite film properties and cost reduction. Furthermore, the precise mechanism for *in situ* CaCO₃ precipitation on RC films is still ambiguous.

The properties of a biocomposite made of RC by NaOH/urea solution and *in situ* calcium carbonate precipitation remains to be elucidated. In this study, strong and translucent RC biocomposite films filled with calcium carbonate were developed. The method involved the coagulation and regeneration of cellulose films and *in situ* calcium carbonate precipitation in the regenerated hydrogel. The properties of RC and calcium carbonate biocomposite films were evaluated. The starting materials were also characterized. The effects of the precursor concentration on the properties of the biocomposite films are discussed.

EXPERIMENTAL

Materials and Chemicals

Cellulose powder from cotton linters was purchased from Hubei Chemical Fiber Group Co., Ltd. (Xiangyang, China) and milled to pass through a 40-mesh sieve with a laboratory grinder (FZ102; Tianjin Taipingyuanda Instrument Co., Ltd., Tianjin, China). The molecular weight of cellulose was estimated to be 1.07×10^5 kg/mol by using a viscometer. Calcium chloride and sodium carbonate were obtained from Sigma-Aldrich (Shanghai, China). Sodium hydroxide, urea, and sulfuric acid were obtained from Sinopharm Chemical Reagent Co., Ltd. (Shanghai, China) and used as received.

Cellulose Dissolution with NaOH/Urea Solution

Cellulose powder was dried at 80 °C for 6 h in a vacuum drying oven (BPZ-6033; Shanghai Yiheng Scientific Instrument Co., Ltd., Shanghai, China). Cellulose solvent, NaOH/urea solution, was made by mixing NaOH, urea, and H₂O at a weight ratio of 7 : 12 : 81. The NaOH/urea solution was precooled to -12 °C in a refrigerator (SC-276; Haier Company Limited, Qingdao, China). A 4.0 wt% suspension of cellulose powder in NaOH/urea solution was made by dissolving 4 g of cotton linters powder in 96 g NaOH/urea solution. The suspension was vigorously stirred for 5 min. The air bubbles and undissolved cellulose aggregates were removed by centrifuge with an Avanti J-E Centrifuge (JA-10 rotor; Beckman Coulter, Brea, CA, USA) at 8000 rpm for 10 min. A transparent and viscous cellulose solution was obtained.

Preparation of RC Film *via* Solution Casting

Cellulose solution was poured onto a glass plate and cast with a glass rod. The glass rod wrapped with a certain thickness tape evenly distributed the cellulose solution. A layer of hydrogel with thickness proportional to the tape thickness was formed. The glass plate with the cellulose hydrogel was gently placed into a coagulation bath (1 L 5% H₂SO₄) until the film was detached from the plate, which took approximately 5 min. The detached film was carefully washed with deionized water (DI) until the pH of water did not change. The film was then air-dried on a stainless steel plate surface. The obtained film was labeled as RC and kept for further analysis.

Preparation of RC Film with *in-situ* CaCO₃ Precipitation

In-situ precipitation of calcium carbonate into RC film was performed by sequentially impregnating calcium chloride and sodium carbonate in the presence of RC film. In detail, the RC hydrogel film was firstly immersed in calcium chloride solution at concentrations of 0.2, 0.5, 0.8, or 1.0 mol/L for 24 h. Then, the hydrogel film was immersed in a sodium carbonate solution of the same concentration as the calcium chloride solution for another 24 h. Calcium carbonate can be obtained through the double-exchange reaction between sodium carbonate and calcium chloride. The RC with *in-situ* CaCO₃ precipitation was gently washed with DI water and air-dried. The films were labeled as RC-C02, RC-C05, RC-C08, and RC-C10, depending on the concentration of the solution for CaCO₃ formation.

Methods

Light transmittance and optical properties of RC were determined by a conventional UV-visible (UV-vis) spectrometer (DU800; Beckman Coulter, Brea, CA, USA) in the range of 200 to 800 nm with air as the background. A wavelength of 600 nm was used to determine the film transmittance. Each sample was scanned three times. The tensile strength of RC films was measured with a tensile tester (Model YG026MB; Fangyuan Instrument Co., Ltd., Wenzhou, China) with a 1000-N load cell at a speed of 5 mm/min at 26 °C and 65% relative humidity. At least five specimens were measured for each sample, and the average value was reported. Surface and cross-section morphologies of RC films were determined using an S-3400N scanning electron microscope (SEM) equipped with an EDAX energy-dispersive X-ray (EDAX LLC, Mahwah, NJ, USA). The specimens were carefully mounted on an SEM sample stub with double-sided sticky carbon conductive tape and then spray coated with gold (MSP-1S; Shinkku VD, Tokyo, Japan) for 60 s in a vacuum chamber before analysis. The energy-dispersive X-ray spectrum was conducted to confirm

the presence of CaCO_3 in RC film. The X-ray diffraction (XRD) spectra of RC films were analyzed using a D8 Advance diffractometer with a $\text{CuK}\alpha$ source (Bruker AXS, Billerica, MA, USA). Scans with an angle range of $2\theta = 10$ to 60° were collected with a speed of $2^\circ/\text{min}$. Fourier transform infrared spectroscopy (FTIR) spectra were determined using a Nexus 470 FTIR spectrometer (Thermo Electron Corporation, Waltham, MA, USA). The RC film was first dried and milled into fine powder in liquid nitrogen. Samples were then mixed with KBr and pelletized into a transparent pallet, and their spectra in the range of 4000 to 500 cm^{-1} with a resolution of 4 cm^{-1} were recorded. Thermogravimetric analyses (TGA) were conducted to examine the degradation behavior of the RC at various CaCO_3 precipitation using a thermogravimetric analyzer (TGA 4000; Perkin Elmer, Waltham, MA, USA). Approximately 5 mg specimens were heated at $10\text{ }^\circ\text{C}/\text{min}$ from $30\text{ }^\circ\text{C}$ to $800\text{ }^\circ\text{C}$ in a nitrogen atmosphere ($50\text{ mL}/\text{min}$).

RESULTS AND DISCUSSION

Optical Transmittance and Tensile Strength of RC- CaCO_3 Films

The RC biocomposite films prepared by solution casting and *in situ* CaCO_3 precipitation had good flexibility. Figure 1a to 1e show optical images of the RC films with CaCO_3 precipitation at concentrations of 0 , 0.2 , 0.5 , 0.8 , and 1.0 mol/L for precursor solutions. The films prepared under different conditions showed obvious differences.

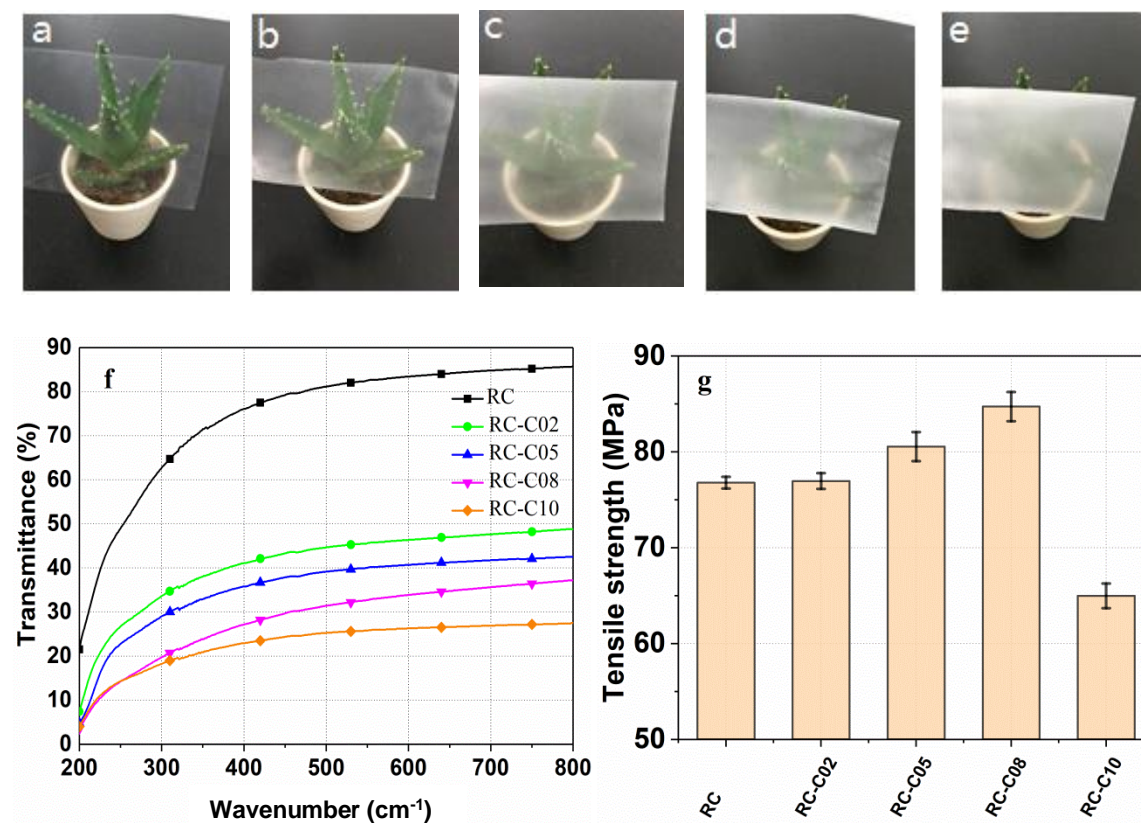


Fig. 1. Visual observation of (a) RC; (b) RC-C02; (c) RC-C05; (d) RC-C08; and (e) RC-C10 e films (thickness = $35\text{ }\mu\text{m}$); (f) UV-Vis spectra of films; and (g) the tensile strength for different samples

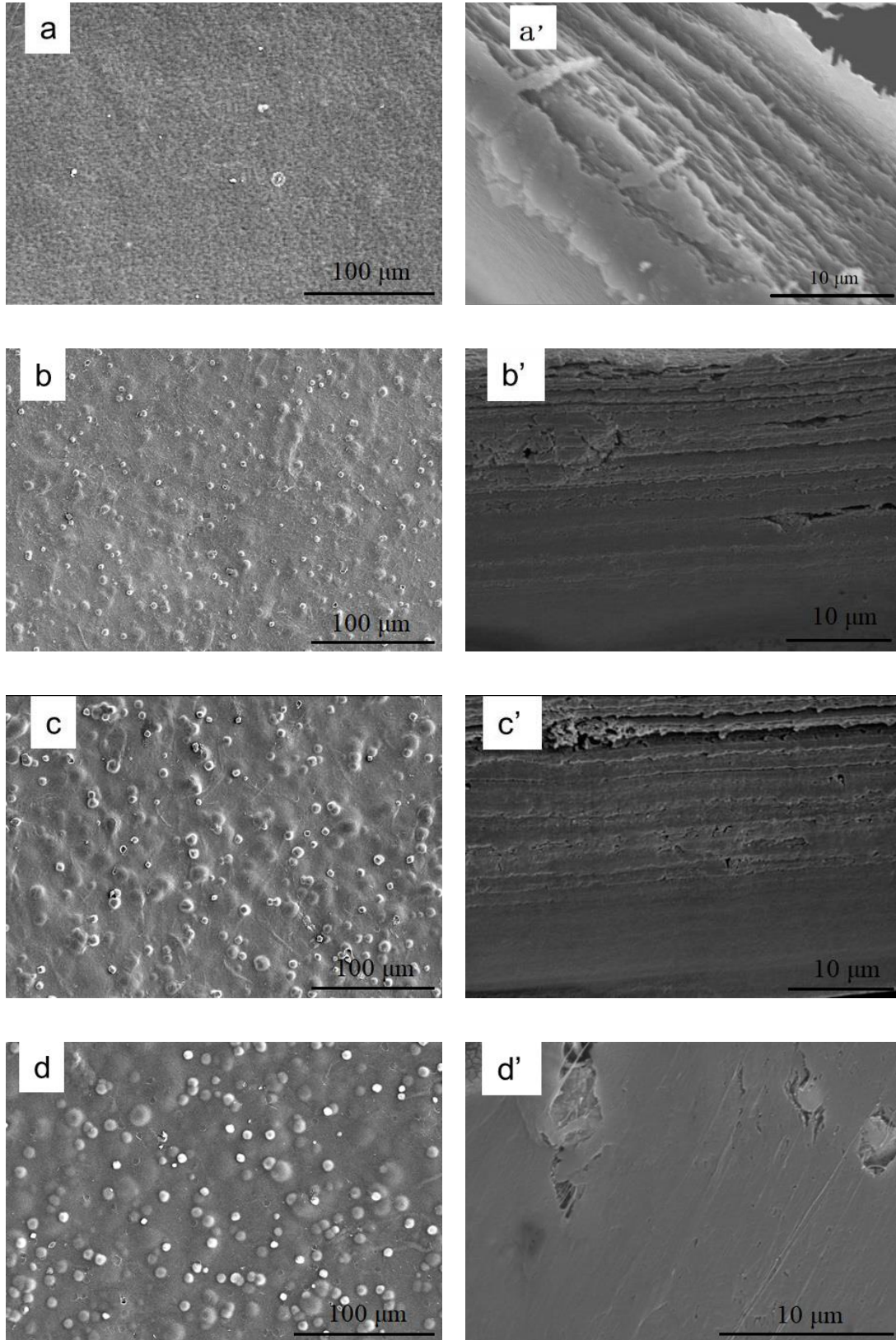
The pure RC film had good transparency, such that the green plant underneath could be seen. The RC-CaCO₃ films were not optically transparent. The transparency of RC-CaCO₃ films decreased with increased precursor in the solutions. The green plant was almost invisible at the highest concentration of calcium carbonate. The RC-CaCO₃ films can be considered as a three-dimensional network structure of RC with micro-nano calcium carbonate particles in between. Because of the inhomogeneous structure in the surface of the composite film, as shown in the SEM image in the following section (Fig. 2), the films exhibited light scattering due to the aggregation of the precipitated calcium carbonate microcrystals (Kumar *et al.* 2011). The change in opacity of the RC-CaCO₃ films can be ascribed to the light absorption and scattering in the gaps between the cellulose fiber and the micro-nano calcium carbonate particles at the interface because the refractive indices of cellulose and CaCO₃ are similar (1.56 to 1.60 vs. 1.58) (Kuo *et al.* 2018; Mohamadzadeh-Saghavaz *et al.* 2014). Translucent or almost opaque films can be achieved depending on the loading of calcium carbonate.

The DU800 UV-Vis spectrophotometer was used for quantitative analysis of the light transmittance of the films, as shown in Fig. 1f. The RC film had the highest transparency in the UV-visible region, which was above 70% transmittance. As the content of calcium carbonate increased, the transparency of films was gradually reduced in both UV and visible light range due to the light scattering (Kumar, *et al.* 2011).

The tensile strength of the films was measured, and the results are displayed in Fig. 1g. The films prepared from pure RC exhibited an average tensile strength of 76.8 MPa. It was reported that the degree of polymerization (DP) of RC did not change much after dissolution and regeneration processes, which may be responsible for the high strength (Cai *et al.* 2004, 2007). No obvious difference in tensile strength can be observed for the film at low calcium carbonate loading (RC-C02). The tensile strength of the films was greatly enhanced by the increasing calcium carbonate loading (Choi *et al.* 2018; Seo *et al.* 2014), which had an average tensile strength of 80.5 and 84.7 MPa for RC-05 and RC-08, respectively. Further increasing the calcium carbonate content not only did not increase the tensile strength but made it lower than the neat RC film. It was estimated that the voids of RC film were filled with calcium carbonate at low calcium carbonate loading, which may contribute to the tensile strength of films. However, with the further increase in calcium carbonate loading, the weak interactions between cellulose fibrils and calcium carbonate may undermine the tensile strength.

SEM Morphology of RC-CaCO₃ Films

The morphological changes of surfaces and cross-sections of the films with different calcium carbonate loading were evident from SEM images in Fig. 2. The pure RC film exhibited a fibrous network structure with a smooth surface, as shown in Figs. 2a and 2a'. This porous RC network structure could provide large amounts of nucleation sites for the *in-situ* calcium carbonate formation process. The SEM images evidenced the presence of calcium carbonate crystals within both surface and cross-section of the films. The results indicated that the crystallization of CaCO₃ occurred with cellulose surrounding. The small size of visible surface crystals of precipitated calcium carbonate appeared in the RC-C02 specimen, which was prepared with the lowest concentration for *in situ* precipitation. The precipitated calcium carbonate with the largest size was detected in the RC-C10 film. The SEM images of the cross-section of films showed that CaCO₃ filled up the network structure.



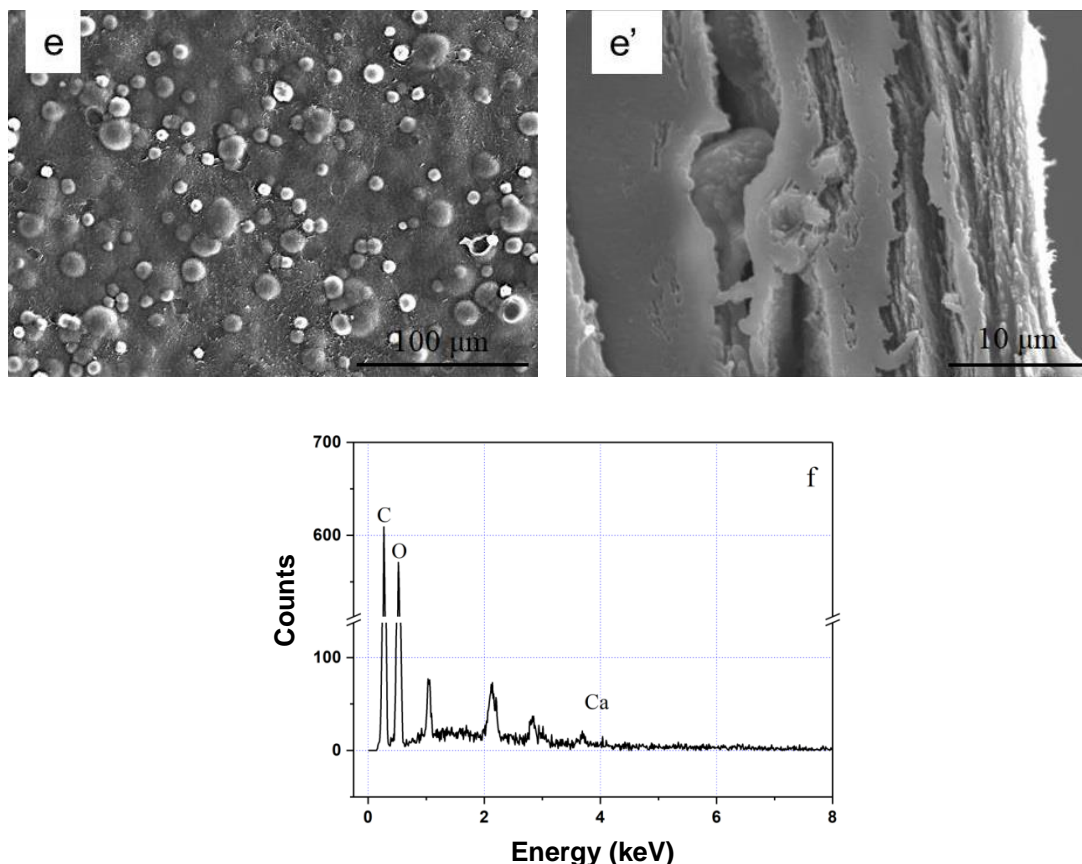


Fig. 2. SEM images of the RC-CaCO₃ films prepared by *in situ* precipitation with different concentrations of precursor solutions (a, a') RC; (b, b') RC-C02; (c, c') RC-C05; (d, d') RC-C08; (e, e') RC-C10; (f) EDS spectrum of RC-C02

Calcium carbonate particles had a smaller size and a high presence within the network pores, indicating that precipitation occurred mainly within the RC network structures. Thanks to the dense *in-situ* precipitation of micro-nanosized CaCO₃ particles, fibrous structures could no longer be observed. It was reported that the regenerated hydrogel experienced crystallization pressure during the CaCO₃ crystal growth (Rauch *et al.* 2012). The crystallization pressures were relatively weak compared to the strong RC network structure at a low concentration of precursor solution. When the concentration of the precursor solution was increased, the crystallization pressures pushed the RC fiber away, as shown in Figs. 2b' and 2c'. Layered structures without voids were observed in RC-C02 and RC-C05, which may be responsible for the high tensile strength. Further increase in the crystallization pressures resulted in the densely packed RC-C08 structure. The RC-C10 films presented large voids due to the crystallization pressure that pushed the RC network fibril away as discussed above. The collapse of the densely packed structure resulted in a decrease in tensile strength. Furthermore, as shown in Fig. 2g, energy dispersive X-ray spectroscopy (EDS) signals of C, O, and Ca elements confirmed the presence of CaCO₃ in the films (Fu *et al.* 2014; Hafez *et al.* 2020).

XRD Analysis of RC-CaCO₃ Films

The incorporation of CaCO₃ in the film was further recognized by the XRD pattern measurement, which is shown in Fig. 3. As a comparison, the pattern of the precipitated calcium carbonate was also supplied in which characteristic peaks corresponded to the

structure of calcite. The XRD peaks located at 2θ values of 23.1° , 29.6° , 36.4° , 39.8° , 43.6° , 47.8° , and 48.9° can be assigned to (102), (104), (110), (113), (202), (108), and (116) planes of calcite (Saraya and Rokbaa 2016). The diffraction pattern of the RC film showed three major characteristic peaks of cellulose II structure at $2\theta = 12.0^\circ$, 20.0° , and 22.5° , which corresponded to the $(1\bar{1}0)$, (110), and (020) planes, respectively (Qi *et al.* 2009; Li *et al.* 2015). The XRD pattern of the RC-C05 film was quite similar to the pattern of the RC film. The differences between them were evident in weakened peaks at $2\theta = 20.0^\circ$ and 22.5° , corresponding to the crystalline cellulose II (110) and (020) plane, and a new peak for (104) plane of calcite (Rauch *et al.* 2012). The less intense and broader peaks for cellulose II in the RC-CaCO₃ composite indicated that the precipitated CaCO₃ generated a further disordered arrangement of cellulose chains. Only the (104) plane of calcite was found in the XRD pattern. Other characteristic peaks of calcite were missing, which may be due to the low crystallinity of calcite in the composite (Niu *et al.* 2014; Xu *et al.* 2017). Overall, XRD results indicated the successful *in-situ* precipitation of calcite into the RC film.

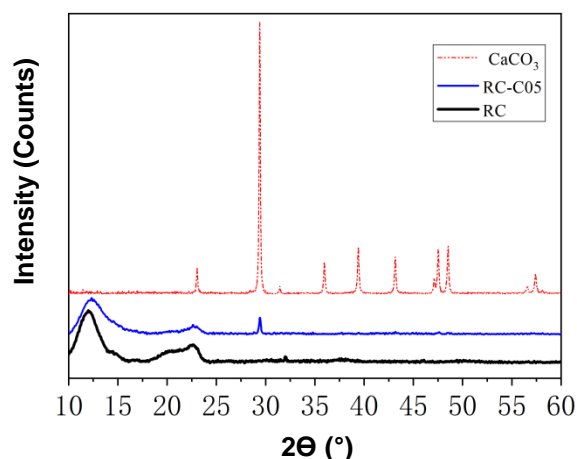


Fig. 3. X-ray diffractograms of RC film, RC-C05 films, and CaCO₃

To gain an insight into the effect of *in-situ* CaCO₃ precipitation on the modulation of the RC film structure, the precipitated CaCO₃ crystal structure, RC film, and RC-CaCO₃ films were also characterized by FTIR and the spectra are shown in Fig. 4. From the FTIR spectrum of the precipitated CaCO₃, it can be seen that CaCO₃ had adsorption bands at 1459 , 875 , and 714 cm^{-1} corresponding to the stretching vibration of the O-C-O bond, the bending vibration in the O-C-O plane, and the out plane bending vibration, respectively. They all were characteristic peaks in the most stable polymorph of CaCO₃ (calcite) (Nelson and Featherstone 1982; Swain *et al.* 2014).

FTIR Analysis of RC-CaCO₃ Films

As shown from the spectrum of pure RC film, typical characteristic peaks of cellulose were observed at 1060 , 1426 , 2900 , and 3403 cm^{-1} (Wang *et al.* 2015). The band at 1060 cm^{-1} corresponded to the stretching vibration peak of the ether bond COC. The presence of the band at 1426 cm^{-1} was due to the shear vibration of the -CH₂ group. The band at 1659 cm^{-1} may attributed to the OH bending of absorbed water. The band at 2900 cm^{-1} was attributed to the stretching vibration of CH in the -CH₂ group. A wide characteristic absorption peak appearing at a position near 3403 cm^{-1} was the stretching vibration peak of -OH. A moderate intensity band at 1459 cm^{-1} , assigned to calcite,

indicated the successful CaCO_3 incorporation in the biocomposite network. Moreover, the absorption peak at 714 cm^{-1} also confirmed the presence of CaCO_3 in the films. For RC- CaCO_3 films, the -OH peaks near 3340 cm^{-1} broadened and moved to the low wave direction, which may indicate the formation of new hydrogen bonding between cellulose and calcium carbonate (Ma *et al.* 2016).

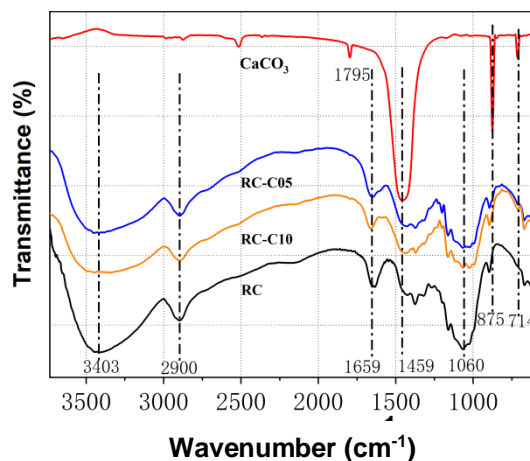


Fig. 4. FTIR of RC and RC- CaCO_3 films

Thermal Analysis RC- CaCO_3 Films

The thermal properties of RC- CaCO_3 were examined by TGA. The TGA results of RC film, CaCO_3 , and RC- CaCO_3 in the temperature range from 30 to $850\text{ }^\circ\text{C}$ are compared in Fig. 5. Only one weight loss region in the range of 600 to $750\text{ }^\circ\text{C}$ was observed during the decomposition of calcium carbonate. The measured value of weight left for CaCO_3 after decomposition (56.5%) was almost the same as the theoretical value (56.1%). The TGA curve of the RC film exhibited a small weight loss in the region from room temperature to $150\text{ }^\circ\text{C}$ due to the loss of moisture in the films. Following this, a two-stage degradation of RC film was located at roughly $250\text{ }^\circ\text{C}$ to $380\text{ }^\circ\text{C}$ and $400\text{ }^\circ\text{C}$ to $700\text{ }^\circ\text{C}$, respectively (Zhu *et al.* 2020c). The first step decomposition region was attributed to the loss of the glycosidic bonds of cellulose, while the second stage, for the RC- CaCO_3 film, it was related to further degradation of cellulose and CaCO_3 in the films (Jia *et al.* 2012; Fu *et al.* 2014). The thermal decomposition curve of RC- CaCO_3 displayed the same trend as that of pure RC films. However, some visible differences between the neat RC film and RC- CaCO_3 films in the two major decomposition regions were detected. It was noteworthy that the decomposition temperature for the RC- CaCO_3 film was slightly lower than that of pure RC film. The reason for TGA curve deviation may arise from the differences in the film structures and processing histories. Further studies are required to explain this early decomposition. A similar trend for the thermal degradation curve of the composite with low CaCO_3 loading was also reported (Ummartyotin *et al.* 2016).

In the pure RC film, char residue was approximately 3.7% at $800\text{ }^\circ\text{C}$. The RC- CaCO_3 films presented residues of 4.6%, 8.8%, and 12.7% for RC-C05, RC-C08, and RC-C10, respectively, confirming the CaCO_3 incorporation within the RC matrix. The CaCO_3 content in the films could be estimated as the difference between the residue from pure RC film and RC- CaCO_3 films (Mohammadkazemi *et al.* 2016). Taking this into account, the estimated CaCO_3 contents for RC-C05, RC-C08, and RC-C10 films were 1.7%, 9.7%, and 17.0%, respectively.

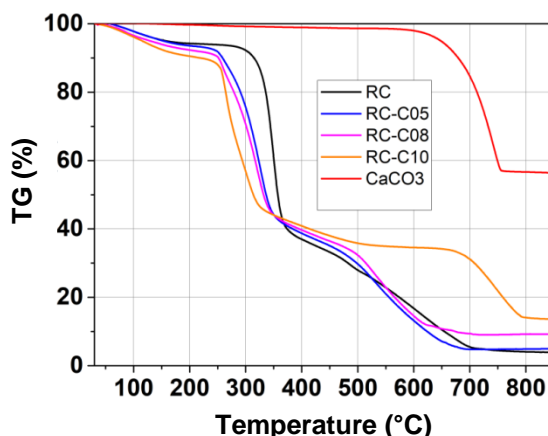


Fig. 5. TGA curves of the CaCO_3 , RC film, and biocomposites

CONCLUSIONS

1. Fully renewable RC- CaCO_3 biocomposite films were successfully synthesized by *in situ* precipitation of CaCO_3 . The results indicated that CaCO_3 was successfully introduced into the RC matrix. The XRD results indicated that the most stable CaCO_3 phase, calcite, was formed during *in situ* precipitation.
2. The properties of the biocomposite films changed as the calcium carbonate content varied. The biocomposites exhibited partial declines in transparency due to the light scattering of CaCO_3 particles. The agglomerations of calcium carbonate on the surface of the films resulted in low transparency.
3. As calcium carbonate content increased, the tensile strength was first increased and then decreased. The RC-C08 film achieved the highest tensile strength of 84.7 MPa. The condensed layer structure may explain the increase in the tensile strength. The RC- CaCO_3 biocomposite films fabricated in this study can be regarded as a green biomaterial with large possibilities of being widely used in packaging and other applications.

ACKNOWLEDGMENTS

This work was supported by the National Key R&D Program of China (2018YFE0107100), the State Key Laboratory of Pulp and Paper Engineering (202003), South China University of Technology, the Key Laboratory of Biomass Energy and Material of Jiangsu Province (JSBEM202012), Institute of Chemical Industry of Forest Products, Chinese Academy of Forestry, and Jiangsu University self-made experimental equipment funding (5623080004).

REFERENCES CITED

- Cai, J., Zhang, L., Zhou, J., Li, H., Chen, H., and Jin, H. (2004). "Novel fibers prepared from cellulose in NaOH/urea aqueous solution," *Macromolecular Rapid Communications* 25(17), 1558-1562. DOI: 10.1002/marc.2004000172
- Cai, J., Zhang, L., Zhou, J., Qi, H., Chen, H., Kondo, T., Chen, X., and Chu, B. (2007). "Multifilament fibers based on dissolution of cellulose in NaOH/urea aqueous solution: Structure and properties," *Advanced Materials* 19(6), 821-825. DOI: 10.1002/adma.200601521
- Cheng, X. F., Qian, H., Zhang, S. W., Zhang, Z. S., He, Y., and Ma, M. G. (2016). "Preparation and characterization of cellulose-CaCO₃ composites by an eco-friendly microwave-assisted route in a mixed solution of ionic liquid and ethylene glycol," *BioResources* 11(2), 4392-4401. DOI: 10.15376/biores.11.2.4392-4401
- Choi, J. S., Kang, D. S., Han, J. S., and Seo, Y. B. (2018). "Property development mechanism of hybrid calcium carbonate," *ACS Sustainable Chemistry & Engineering* 7(1), 1538-1544. DOI: 10.1021/acssuschemeng.8b05304
- Ciobanu, M., Bobu, E., and Ciolacu, F. (2010). "In-situ cellulose fibres loading with calcium carbonate precipitated by different methods," *Cellulose Chemistry and Technology* 44(9), 379-387.
- Delhom, C. D., White-Ghoorahoo, L. A., and Pang, S. S. (2010). "Development and characterization of cellulose/clay nanocomposites," *Composites Part B: Engineering* 41(6), 475-481. DOI: 10.1016/j.compositesb.2009.10.007
- Fu, L. H., Ma, M.-G., Bian, J., Deng, F., and Du, X. (2014). "Research on the formation mechanism of composites from lignocelluloses and CaCO₃," *Materials Science and Engineering: C* 44, 216-224. DOI: 10.1016/j.msec.2014.08.029
- Hafez, I., Amini, E., and Tajvidi, M. (2020). "The synergy between cellulose nanofibrils and calcium carbonate in a hybrid composite system," *Cellulose* 27(7), 3773-3787. DOI: 10.1007/s10570-020-03032-w
- Jia, N., Li, S. M., Ma, M. G., Sun, R. C., and Zhu, J. F. (2012). "Hydrothermal fabrication, characterization, and biological activity of cellulose/ CaCO₃ bionanocomposites," *Carbohydrate Polymers* 88(1), 179-184. DOI: 10.1016/j.carbpol.2011.11.086
- Kumar, N., Bhardwaj, N. K., and Chakrabarti, S. K. (2011). "Influence of particle size distribution of calcium carbonate pigments on coated paper whiteness," *Journal of Coatings Technology and Research* 8(5), Article number 613. DOI: 10.1007/s11998-011-9353-y
- Kuo, D., Nishimura, T., Kajiyama, S., and Kato, T. (2018). "Bioinspired environmentally friendly amorphous CaCO₃-based transparent composites comprising cellulose nanofibers," *ACS Omega* 3(10), 12722-12729. DOI: 10.1021/acsomega.8b02014
- Laukala, T., Kronlund, D., Heiskanen, I., and Backfolk, K. (2017). "The effect of polyacrylic acid and reaction conditions on nanocluster formation of precipitated calcium carbonate on microcellulose," *Cellulose* 24(7), 2813-2826. DOI: 10.1007/s10570-017-1296-8
- Li, R., Wang, S., Lu, A., and Zhang, L. (2015). "Dissolution of cellulose from different sources in an NaOH/urea aqueous system at low temperature," *Cellulose* 22(1), 1-11. DOI: 10.1007/s10570-014-0542-6

- Ma, M. G., Liu, S., and Fu, L. H. (2016). "Calcium carbonate and cellulose/calcium carbonate composites: Synthesis, characterization, and biomedical applications," *Materials Science Forum* 875, 24-44. DOI: 10.4028/www.scientific.net/MSF.875.24
- Mohamadzadeh-Saghavaz, K., Resalati, H., and Ghasemian, A. (2014). "Cellulose-precipitated calcium carbonate composites and their effect on paper properties," *Chemical Papers* 68(6), 774-781. DOI: 10.2478/s11696-013-0513-7
- Mohammadkazemi, F., Faria, M., and Cordeiro, N. (2016). "In situ biosynthesis of bacterial nanocellulose- CaCO₃ hybrid bionanocomposite: One-step process," *Materials Science and Engineering: C* 65, 393-399. DOI: 10.1016/j.msec.2016.04.069
- Nakao, Y., Sugimura, K., and Nishio, Y. (2019). "CaCO₃ mineralization in polymer composites with cellulose nanocrystals providing a chiral nematic mesomorphic structure," *International Journal of Biological Macromolecules* 141, 783-791. DOI: 10.1016/j.ijbiomac.2019.09.045
- Nelson, D., and Featherstone, J. (1982). "Preparation, analysis, and characterization of carbonated apatites," *Calcified Tissue International* 34, S69-81.
- Niu, T., Xu, J., and Huang, J. (2014). "Growth of aragonite phase calcium carbonate on the surface of a titania-modified filter paper," *CrystEngComm* 16(12), 2424-2431. DOI: 10.1039/c3ce42322k
- Qi, H., Cai, J., Zhang, L., and Kuga, S. (2009). "Properties of films composed of cellulose nanowhiskers and a cellulose matrix regenerated from alkali/urea solution," *Biomacromolecules* 10(6), 1597-1602. DOI: 10.1021/bm9001975
- Rauch, M. W., Dressler, M., Scheel, H., Van Opdenbosch, D., and Zollfrank, C. (2012). "Mineralization of calcium carbonates in cellulose gel membranes," *European Journal of Inorganic Chemistry* 2012(32), 5192-5198. DOI: 10.1002/ejic.201200575
- Saito, T., Oaki, Y., Nishimura, T., Isogai, A., and Kato, T. (2014). "Bioinspired stiff and flexible composites of nanocellulose-reinforced amorphous CaCO₃," *Materials Horizons* 1(3), 321-325. DOI: 10.1039/c3mh00134b
- Saraya, M. E. S. I., and Rokbaa, H. (2016). "Preparation of vaterite calcium carbonate in the form of spherical nano-size particles with the aid of polycarboxylate superplasticizer as a capping agent," *American Journal of Nanomaterials* 4(2), 44-51. DOI: 10.12691/ajn-4-2-3
- Sathitsuksanoh, N., George, A., and Zhang, Y. H. P. (2013). "New lignocellulose pretreatments using cellulose solvents: A review," *Journal of Chemical Technology and Biotechnology* 88(2), 169-180. DOI: 10.1002/jctb.3959
- Seo, Y. B., Ahn, J. H., and Lee, H. L. (2017). "Upgrading waste paper by in-situ calcium carbonate formation," *Journal of Cleaner Production* 155(Part 1), 212-217. DOI: 10.1016/j.jclepro.2016.09.003
- Seo, Y. B., Lee, Y. H., and Chung, J. K. (2014). "The improvement of recycled newsprint properties by in-situ CaCO₃ loading," *BioResources* 9(4), 6254-6266. DOI: 10.15376/biores.9.4.6254-6266
- Swain, S. K., Dash, S., Kisku, S. K., and Singh, R. K. (2014). "Thermal and oxygen barrier properties of chitosan bionanocomposites by reinforcement of calcium carbonate nanopowder," *Journal of Materials Science & Technology* 30(8), 791-795. DOI: 10.1016/j.jmst.2013.12.017
- Ummartyotin, S., Pisitsak, P., and Pechyen, C. (2016). "Eggshell and bacterial cellulose composite membrane as absorbent material in active packaging," *International Journal of Polymer Science* 2016, Article ID 1047606. DOI: 10.1155/2016/1047606

- Wang, Q., Wei, W., Kingori, G. P., and Sun, J. (2015). "Cell wall disruption in low temperature NaOH/urea solution and its potential application in lignocellulose pretreatment," *Cellulose* 22(6), 3559-3568. DOI: 10.1007/s10570-015-0767-z
- Wang, Q., Wei, W., Li, X., Sun, J., He, J., and He, M. (2016). "Comparative study of alkali and acidic cellulose solvent pretreatment of corn stover for fermentable sugar production," *BioResources* 11(1), 482-491. DOI: 10.15376/biores.11.1.482-491
- Wang, Q., Yao, Q., Liu, J., Sun, J., Zhu, Q., and Chen, H. (2019). "Processing nanocellulose to bulk materials: A review," *Cellulose* 26(13-14), 7585-7617. DOI: 10.1007/s10570-019-02642-3
- Wang, Q. Q., Sun, J. Z., Yao, Q., Ji, C. C., Liu, J., and Zhu, Q. Q. (2018). "3D printing with cellulose materials," *Cellulose* 25(8), 4275-4301. DOI: 10.1007/s10570-018-1888-y
- Xiao, W., Liu, J., Chen, Q., Wu, Y., Dai, L., and Wu, T. (2011). "Controllable mineralization of calcium carbonate on regenerated cellulose fibers," *Crystal Research and Technology* 46(10), 1071-1078. DOI: 10.1002/crat.201100261
- Xu, Y. J., Jiang, C. M., Duan, C., and Zhang, W. P. (2017). "In-situ preparation of nano-calcium carbonate/cellulose fiber composite and its application in fluff pulp," *Journal of Engineered Fibers and Fabrics* 12(3), 48-53. DOI: 10.1177/155892501701200306
- Yang, Q., Wu, C. N., Saito, T., and Isogai, A. (2014). "Cellulose-clay layered nanocomposite films fabricated from aqueous cellulose/LiOH/urea solution," *Carbohydrate Polymers* 100, 179-184. DOI: 10.1016/j.carbpol.2012.10.044
- Zhu, Q., Liu, S., Sun, J., Liu, J., Kirubakaran, C. J., Chen, H., Xu, W., and Wang, Q. (2020a). "Stimuli-responsive cellulose nanomaterials for smart applications," *Carbohydrate Polymers* 235, Article ID 115933. DOI: 10.1016/j.carbpol.2020.115933
- Zhu, Q., Wang, J., Sun, J., and Wang, Q. (2020b). "Preparation, characterization, and oxygen barrier properties of regenerated cellulose/polyvinyl alcohol blend films," *BioResources* 15(2), 2735-2746. DOI: 10.15376/biores.15.2.2735-2746
- Zhu, Q., Yao, Q., Sun, J., Chen, H., Xu, W., Liu, J., and Wang, Q. (2020c). "Stimuli induced cellulose nanomaterials alignment and its emerging applications: A review," *Carbohydrate Polymers* 230, Article ID 115609. DOI: 10.1016/j.carbpol.2019.115609

Article submitted: June 20, 2020; Peer review completed: August 15, 2020; Revised version received: August 17, 2020; Accepted: August 18, 2020; Published: August 31, 2020.

DOI: 10.15376/biores.15.4.7893-7905